Towards a multi-platform assimilative system for ocean biogeochemistry

Jozef Skákala[1,2], David Ford[3], Jorn Bruggeman[1], Tom Hull[4,5], Jan Kaiser[5], Robert R. King[3], Benjamin Loveday[1], Matthew R. Palmer[6], Tim Smyth[1], Charlotte Williams[6]and Stefano Ciavatta[1,2]

[1]Plymouth Marine Laboratory, The Hoe, Plymouth, PL1 3DH United Kingdom.
[2]National Centre for Earth Observation, Plymouth, PL1 3DH, UK.
[3]Met Office, FitzRoy Road, Exeter, EX1 3PB UK.
[4]Centre for Environment, Fisheries and Aquaculture Science, Lowestoft, NR33 0HT UK.
[5]Centre for Ocean and Atmospheric Sciences, University of East Anglia, Norwich, NR4 7TJ, UK.
[6]National Oceanography Centre, Joseph Proudman Building, 6 Brownlow Street, Liverpool, L3 5DA UK.

Key Points:

- We developed a skilled multi-platform assimilative system for biogeochemistry in the North Sea.
- We tested the impact of the different assimilative system components on the ecosystem reanalysis.
- The multi-platform assimilation will become an essential part of future operational research.

Corresponding author: Jozef Skákala, jos@pml.ac.uk

Abstract

Oceanography has entered an era of new observing platforms, such as biogeochemical Argo floats and gliders, some of which will provide three-dimensional maps of essential ecosystem variables on the North-West European (NWE) Shelf. In a foreseeable future operational centres will use multi-platform assimilation to integrate those valuable data into ecosystem reanalyses and forecast systems. Here we address some important questions related to glider biogeochemical data assimilation and introduce multi-platform data assimilation in a (pre)operational model of the NWE Shelf-sea ecosystem. We test the impact of the different multi-platform system components (glider vs satellite, physical vs biogeochemical) on the biogeochemical model skill. To characterize the model skill we focus on the period around the phytoplankton spring bloom, since the bloom is a major ecosystem driver on the NWE Shelf. We found that the timing and magnitude of the phytoplankton bloom is insensitive to the temperature and salinity glider assimilation, which is explained in the study. To correct the simulated phytoplankton bloom one needs to assimilate chlorophyll observations from glider or satellite Ocean Color (OC) into the model. Although glider chlorophyll assimilation outperforms OC assimilation, we show that OC assimilation has a capability to correct the vertical chlorophyll profiles. Since the OC assimilation updates chlorophyll only in the mixed layer, improvements in the simulation of the chlorophyll vertical profiles are the result of the model dynamical response to the assimilation. We demonstrate that the multi-platform assimilation combines the advantages of its components and always performs comparably to its best performing component.

1 Introduction

Understanding the state and the future of shelf-sea ecosystems is essential from the point of view of economy, conservation and the global carbon cycle (*Pauly et al.* [2002]; *Borges et al.* [2006]; *Friedlingstein et al.* [2006]; *Jahnke* [2010]). Reanalyses provide our best estimate of the ocean state by optimally combining the state-of-the-art knowledge from models with the most up-to-date observations. In marine biogeochemistry the prevailing approach is to assimilate into models the satellite products, either for Ocean Color (OC) derived total chlorophyll (e.g *Ishizaka* [1990]; *Carmillet et al.* [2001]; *Natvik and Evensen* [2003]; *Hoteit et al.* [2005]; *Triantafyllou et al.* [2007]; *Nerger and Gregg* [2007, 2008]; *Gregg* [2008]; *Fontana et al.* [2010]; *Ford et al.* [2012]; *Ciavatta et al.* [2011, 2016]; *Kalaroni et al.* [2016]; *Ford and Barciela* [2017]; *Pradhan et al.* [2019]), Phytoplankton Functional Type (PFT)-specific chlorophyll (*Ciavatta et al.* [2018, 2019]; *Skákala et al.* [2018, 2020]), or surface radiances (*Shulman et al.* [2013]; *Ciavatta et al.* [2014]; *Jones et al.* [2016]; *Gregg and Rousseaux* [2017]; *Skákala et al.* [2020]). Additionally a number of studies assimilated biogeochemical data from in situ measurements, either using single-location profiles (e.g. *Allen et al.* [2003]; *Hoteit et al.* [2003]; *Torres et al.* [2006]; *Lenartz et al.* [2007]), or using surface data from ships, floats and buoys (e.g *Anderson et al.* [2000]; *Cossarini et al.* [2009]; *Song et al.* [2016]). The typical disadvantage of the traditionally assimilated biogeochemical data-sets is that they are either constrained to the ocean surface (e.g. in the case of satellite data), or they are typically limited to a single location (in the case of vertically-measured data). Assimilating such data into the model has either only local impact, or its impact on biogeochemical fields is typically constrained to the upper oceanic layer, with uncertain impact on the vertical profiles of biomass, or nutrients.

However, the situation on the data-front is rapidly changing, with new programmes (e.g. AtlantOS, *Visbeck et al.* [2015]) aiming at revolutionizing biogeochemical oceanography with novel observing platforms covering large parts of the ocean both horizontally and vertically, such as floats deployed in the Biogeochemical-Argo programme (e.g. *Johnson and Claustre* [2016]; *Johnson* [2016]; *Germineaud et al.* [2019]), and gliders with optical and biogeochemical sensors (*Telszewski et al.* [2018]). Some of the Argo float oxygen data were already assimilated to constrain the biogeochemistry in the Southern

Ocean (*Verdy and Mazloff* [2017]) and Argo-measured chlorophyll was assimilated to improve phytoplankton dynamics in the Mediterranean Sea (*Cossarini et al.* [2019]). The new observational activity quite understandably focuses on the regions of high importance for fisheries, economy and climate, such as the North-West European (NWE) Shelf (e.g. *Legge et al.* [2020]), where a number of gliders have been deployed as a part of the Alternative Framework to Assess Marine Ecosystem Functioning in Shelf Seas (AlterECO) programme (*http://projects.noc.ac.uk/altereco/*). The rapid development of these new autonomous observation systems opens up an entirely new range of possibilities on how to optimally integrate multi-platform observing networks with our present oceanographic models (*Lellouche et al.* [2013]; *Bell et al.* [2015]). The observational work on the NWE Shelf from the AlterECO project is coupled to a sister programme, the CAMPUS (Combining Autonomous observations and Models for Predicting and Understanding Shelf seas, *https://www.campus-marine.org/*) project, aiming to consistently combine the different sources of information, such as gliders, satellite OC data and models, in order to improve our capability to understand, represent and forecast the NWE Shelf biogeochemistry (e.g spring bloom, carbon and nutrient cycle, oxygen depletion events). Future plans, based on CAMPUS and in line with the European operational Copernicus Marine Service, are to have a multi-platform assimilative system on the NWE Shelf, where the autonomous vehicles will navigate to specific locations using a combination of Artificial Intelligence (AI) and model forecast, e.g. to detect onset of the phytoplankton bloom, or harmful events.

Trying to establish glider data assimilation as part of such a multi-platform assimilative system often leads to two non-trivial problems: a) how to consistently combine high resolution glider data with much coarser model resolution, b) how to achieve reasonable consistency between the assimilation-corrected variables and the coupled physical-biogeochemical model dynamics. The problem of dynamical consistency needs special mention, since both physical and biogeochemical fields have typically much larger gradients in the vertical than in the horizontal dimension. The vertical correlation length scales have large spatio-temporal variability and model dynamics can be quite sensitive to spurious vertical gradients (*Doney* [1999]; *Oschlies and Garçon* [1999]; *Doney et al.* [2004]). Such model sensitivity is often noticed when physical data (such as sea surface height, or temperature and salinity) are assimilated into the model, as the spurious vertical mixing introduced by such assimilation is known to often degrade the skill of the biogeochemical model (e.g *Berline et al.* [2007]; *While et al.* [2010]; *El Moussaoui et al.* [2011]; *Holt et al.* [2014]; *Raghukumar et al.* [2015]; *Park et al.* [2018]). However, similar issues can be easily overlooked when we assimilate surface biogeochemical data (except extreme regions with substantial small-scale horizontal variability, such as the Gulf Stream, *Anderson et al.* [2000]), since the horizontal distributions of biogeochemical fields are in relative terms smooth and stable. For the gliders, it is of vital interest to understand the potentially complex interaction between the physical and the biogeochemical data assimilation, or the interplay between the different biogeochemical variables updated by the assimilative system.

In this study we extend the operational assimilative system on the NWE Shelf to successfully produce a multi-platform reanalysis (temperature, salinity, total chlorophyll *a*, oxygen from an AlterECO glider and chlorophyll *a* from a satellite OC product). The main focus of the paper is to assess the impact of the different assimilative system components (satellite vs glider, physical vs biogeochemical) on the model skill to simulate ecosystem processes in relation to the phytoplankton spring bloom. Understanding the impact of the different system components is important, since it indicates what will be the reanalysis skill in the regions where only a specific type of data (e.g. satellite OC, physical variables) is available. The focus on the processes around the spring bloom is a natural choice due to a) the availability of high quality chlorophyll glider data, and b) because the spring bloom is on the NWE Shelf a key driver of the ecosystem dynamics (*Lutz et al.* [2007]; *Henson et al.* [2009]). The results of this study should form a basis for the integrated multi-platform assimilative system, that will optimize the available infor-

mation from observations and models in order to improve our understanding of the NWE Shelf biogeochemistry. The paper uses hindcast versions of the operational models for the NWE Shelf run by the Met Office in the framework of the European Copernicus Marine Environment Monitoring Service (CMEMS), i.e. the physical model Nucleus for European Modelling of the Ocean (NEMO, *Madec et al.* [2015]) coupled through the Framework for Aquatic Biogeochemical Models (FABM, *Bruggeman and Bolding* [2014]) with the biogeochemical model European Regional Seas Ecosystem Model (ERSEM, *Baretta et al.* [1995]; *Blackford* [1997]; *Butenschön et al.* [2016]). We used measurements from an AlterEco glider that operated in the central North Sea between May-August 2018 providing data for temperature, salinity, chlorophyll (derived from fluorescence) and oxygen concentrations. In multi-platform assimilation the glider data were complemented with Ocean Color-Climate Change Initiative (OC-CCI) satellite product of the European Space Agency (ESA) for total chlorophyll (version 3.1, *Sathyendranath et al.* [2019]) and assimilated on a daily basis into NEMO-FABM-ERSEM model using NEMOVAR (the assimilative system used operationally by the Met Office, *Mogensen et al.* [2009, 2012]; *Waters et al.* [2015]; *King et al.* [2018]). The assimilated glider variables were selected based on the data availability, but both chlorophyll and oxygen are expected to play an important role in the future multi-platform operational assimilation: chlorophyll is a natural proxy for primary productivity and marine life, while oxygen needs to be monitored and forecast in order to identify oxygen depletion events (hypoxia, *Vaquer-Sunyer and Duarte* [2008]), which can have disastrous impacts on marine life.

2 Methods

2.1 The physical component: Nucleus for European Modelling of the Ocean (NEMO)

The NEMO ocean physics component (OPA) is a finite difference, hydrostatic, primitive equation ocean general circulation model (*Madec et al.* [2015]). The NEMO configuration used in this study is similar to the one used by *Ford et al.* [2017]; *Skákala et al.* [2018], and identical to *Skákala et al.* [2020]: we use the CO6 NEMO version, based on NEMOv3.6, a development of the CO5 configuration explained in detail by *O'Dea et al.* [2017]. The model has 7 km spatial resolution on the Atlantic Margin Model (AMM7) domain using a terrain-following $z^* - \sigma$ coordinate system with 51 vertical levels. The lateral boundary conditions for physical variables at the Atlantic boundary were taken from the outputs of the Met Office $1/12°$ North Atlantic model (NATL12, *King et al.* [2018]); the Baltic boundary values were derived from a reanalysis produced by the Danish Meteorological Institute for the CMEMS. The model (including biogeochemistry) was initialized from the free run of *Skákala et al.* [2020].

As *Skákala et al.* [2020], we use river discharge that has been updated to cover more recent years using data from *Lenhart et al.* [2010]. The model was forced at the surface by atmospheric fluxes provided by a high (hourly) temporal and (31 km) spatial resolution realisation (HRES) of the ERA5 data-set (*https://www.ecmwf.int/*).

2.2 The biogeochemical component: European Regional Seas Ecosystem Model (ERSEM)

ERSEM (*Baretta et al.* [1995]; *Butenschön et al.* [2016]) is a lower trophic level ecosystem model for marine biogeochemistry, pelagic plankton, and benthic fauna (*Blackford* [1997]). The model splits phytoplankton into four functional types largely based on their size (*Baretta et al.* [1995]): picophytoplankton, nanophytoplankton, diatoms and dinoflagellates. ERSEM uses variable stoichiometry for the simulated plankton groups (*Geider et al.* [1997]; *Baretta-Bekker et al.* [1997]) and each Phytoplankton Functional Type (PFT) biomass is represented in terms of chlorophyll, carbon, nitrogen and phosphorus, with diatoms also represented by silicon. ERSEM predators are composed of three zooplankton types (mesozooplankton, microzooplankton and heterotrophic nanoflagellates),

with organic material being decomposed by one functional type of heterotrophic bacteria (*Butenschön et al.* [2016]). The ERSEM inorganic component consists of nutrients (nitrate, phosphate, silicate, ammonium and carbon) and dissolved oxygen. The carbonate system is also included in the model (*Artioli et al.* [2012]).

We used in this study the ERSEM configuration from *Skákala et al.* [2020], based on the model parametrization described in *Butenschön et al.* [2016]. As *Skákala et al.* [2020], the Atlantic boundary values for nitrate, phosphate and silicate were taken from World Ocean Atlas (*Garcia et al.* [2013]) and dissolved inorganic carbon from the GLODAP gridded dataset (*Key et al.* [2015]; *Lauvset et al.* [2016]), while plankton and detritus variables were set to constant values. The ERSEM underwater light field was calculated using a new bio-optical module implemented in the NEMO-FABM-ERSEM AMM7 configuration by *Skákala et al.* [2020]. The bio-optical module resolves light spectrally and distinguishes between downwelling direct and diffuse streams. The module is forced by the ERA5 atmospheric inputs (*https://www.ecmwf.int/*) for total vertically integrated ozone, water vapour, cloud cover, cloud liquid water, sea-level air pressure, as well as by a satellite product for aerosol optical thickness (MODerate resolution Imaging Spectroradiometer, MODIS, *https://modis.gsfc.nasa.gov/data/dataprod*).

2.3 The assimilative system: NEMOVAR

NEMOVAR is a variational Data Assimilation (DA) system (*Mogensen et al.* [2009, 2012]; *Waters et al.* [2015]) used for operational ocean DA at the Met Office. In its biogeochemical applications, assimilating satellite ocean-color derived (PFT) chlorophyll concentrations, NEMOVAR is highly successful in improving the phytoplankton community structure, phytoplankton seasonal cycle, the timing and magnitude of the spring bloom and also the carbon cycle (*Skákala et al.* [2018, 2020]). The 3D-Var version applied in this study uses the First Guess at Appropriate Time (FGAT) approach and minimizes the cost function using the conjugate gradient method (*Mogensen et al.* [2012]). For physics variables, multivariate assimilation is performed as described for the NWE Shelf model by *King et al.* [2018]. For biogeochemical variables, the scheme starts with univariate assimilation of the observed variable. For total chlorophyll the assimilation is applied in log-space, since chlorophyll is typically log-normally distributed (*Campbell* [1995]). After calculating the total chlorophyll increments, we use a balancing module to split those increments into the model state variables. The applied scheme (*Skákala et al.* [2018, 2020]) redistributes total chlorophyll increments into the 4 ERSEM PFTs based on background PFT-to-total chlorophyll ratios. The PFT chlorophyll is used to update the remaining PFT components (carbon, phosphorus, nitrogen for all PFTs, silicon for diatoms) following the background stoichiometric ratios. In the case of oxygen concentration the assimilation is straightforward, as only the ERSEM oxygen variable is updated. There were attempts to extend the currently applied balancing scheme to other ERSEM variables (e.g nutrients), but so-far this produced sub-optimal results degrading the biogeochemical model skill (see discussion in *Skákala et al.* [2018]). Any combined physical-biogeochemical assimilation in NEMOVAR is weakly coupled, which means that the physical and the biogeochemical variables are assimilated separately, with physical assimilation impacting biogeochemistry only through the model dynamics, and no feedback from biogeochemistry to physics.

Satellite OC data assimilation typically uses a "2D method", which consists of a) calculating surface chlorophyll increments and b) propagating those surface increments as constants through the mixed layer. This methodology is applied operationally by the Met Office to assimilate OC data and has been used in *Skákala et al.* [2018, 2020]. Alternatively, surface data can be assimilated similarly to profile data with a "3D variant" based on *Waters et al.* [2015]; *King et al.* [2018]; *Ford* [2020], in which NEMOVAR calculates directly the set of 3D increments using flow-dependent vertical length-scales. The vertical length-scales are based on vertical gradient of water density with the surface length-scale equal to half of the mixed layer depth, decreasing with depth until at half of the mixed

layer depth, while beneath half of the mixed layer depth the length-scales correspond to the local vertical grid resolution. The vertical correlation length-scales are designed to minimise any spurious mixing of surface increments beneath the mixed layer (*King et al.* [2018]). Both 2D and 3D variants were used in this study and we have found that they produced almost identical results (not shown here). In this study we will present the outputs of the 3D variant, but these are representative of both methods.

In this work we use the development from *Ford* [2020] extending the operational NEMOVAR set-up to include assimilation of biogeochemical profiles, as well as combined assimilation of satellite OC and profile data, by following a scheme previously applied to physical variables by *Waters et al.* [2015]. In the multi-platform assimilative system NEMOVAR combines satellite OC and in situ glider chlorophyll to calculate a single set of 3D chlorophyll increments, while allowing for different observation errors to be specified for the different data sources (for the details see *Waters et al.* [2015]; *Ford* [2020]).

The drawback of 3D-Var methods such as NEMOVAR is that the background variances have to be often externally supplied and those do not always capture how the reanalysis approximates the true state. Improvements can be achieved by using hybrid methods (e.g. background variances calculated as a weighted combination of the parameterised component and a flow-dependent component calculated from an ensemble), or iterative methods based on error diagnostics, such as the scheme of *Andersson* [2003]; *Desroziers et al.* [2005]. However, the current NEMOVAR relies on externally supplied variances: the background variances were estimated from the observational-to-free run differences, along the scheme of *Skákala et al.* [2020]. In case of glider data the total observational error (including representation error) was estimated as a difference between true variability and observed variability, where the true variability was estimated from the model outputs. This scheme assumes that (for the limited spatio-temporal range of glider data) the observational errors and the true deviations from the mean are uncorrelated. After estimating the observational errors for gliders, one proceeds with the scheme from *Skákala et al.* [2020] to estimate the corresponding background errors. For both glider and satellite (where the observational errors are provided with the product) the estimated background and observational errors turned out to have comparable values (ratios within 0.5-2). However, for the biogeochemical assimilation at AMM7 using the existing 3D-Var scheme, it has been observed (e.g *Skákala et al.* [2018]) that the reanalysis is relatively insensitive to the precise value of the background-to-observational error ratio. Furthermore, the purpose of this study is to identify and resolve conceptual issues with glider data assimilation, rather than trying to produce the best estimate for the ocean state. The estimates for background and observational errors used in the assimilative runs are therefore deemed sufficient for the goals set in this work.

2.4 Glider data

The study used data from a glider named Cabot deployed during the AlterEco mission (deployment 454). The glider moved in the central North Sea (see Fig.1), between May-August 2018, providing data for temperature, salinity, fluorescence and oxygen. After Quality Control (QC) the quenching-corrected chlorophyll (derived from fluorescence) and oxygen concentrations were available for slightly different periods: chlorophyll for 08/05 - 15/08/2018 and oxygen for a shorter period of 08/05 - 30/06/2018. The Cabot glider was chosen because it provided high-quality data, but the period of the glider mission was also of special interest for assimilation, since it marks a known discrepancy between the timing of the spring bloom in the model and observations, with the model biased towards a late bloom (see *Skákala et al.* [2020]). The QC glider outputs contained a substantial number of data-points ($2 \cdot 10^6$ for chlorophyll and $3 \cdot 10^5$ for oxygen) which were averaged to match the model AMM7 grid on a daily time-scale. The grid-averaging of glider observations is a practice adopted in the physical DA to avoid assimilating many observations at higher resolution than the model can represent. However, our tests have shown that the impact

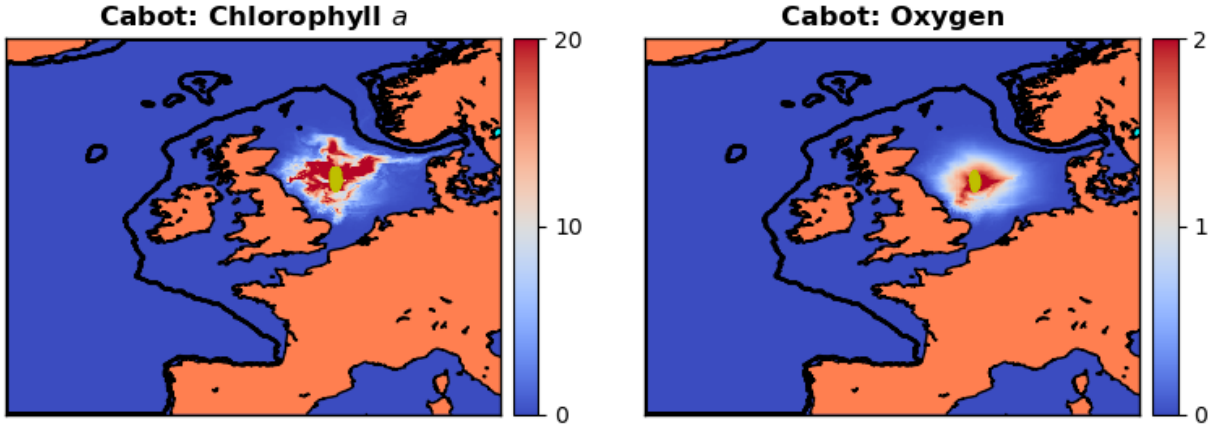

Figure 1. The Figure shows the NEMO-FABM-ERSEM (AMM7) domain with the Cabot glider locations marked by yellow diamonds, as well as glider horizontal area of impact on the reanalysis. The values shown are the weekly (23-29-th June 2018) mean percentage (%) difference between reanalysis and free run in the surface chlorophyll (left) and surface oxygen (right) concentrations. The percentage difference is calculated by dividing the absolute value of the difference between reanalysis and the free run, with the free run. The black lines show the boundary of the NWE Shelf (< 200 m bathymetry).

of grid-averaging on the biogeochemical reanalysis was negligible. During each day the glider typically covered 3 model horizontal grid-cells and for each model horizontal location the glider scanned nearly the full vertical water column.

The glider data (www.bodc.ac.uk) were processed using the GEOMAR slocum glider toolbox which includes a flight model regression and associated lag corrections for temperature, salinity and oxygen. The glider was fitted with a standard non-pumped SBE CT sensor, a WETLabs ECOpuck to measure chlorophyll fluorescence, and an Aanderaa 4330 oxygen optode. Oxygen data were corrected based on comparisons between Winkler samples and local crossings with the rest of the AlterEco glider fleet.

The fluorescence sensor on Cabot (454) was calibrated prior to deployment, and recovered data were converted to chlorophyll concentration from raw voltages using the manufacturer supplied calibration routine. The derived chlorophyll record was filtered such that negative values were set to zero. Multiple quenching corrections were tested, including: *Hemsley et al.* [2015]; *Swart et al.* [2015]; *Biermann et al.* [2015] and *Xing et al.* [2012]. The former three methods rely on the use of algal particle scattering to correct for quenching. However, these approaches proved unsatisfactory for use in case-2 waters (e.g. the North Sea). Consequently, the *Xing et al.* [2012] method was adopted. Under this approach the maximum value of chlorophyll concentration above the mixed layer depth

(MLD) is extrapolated to the surface for daytime profiles. Night-time chlorophyll profiles are not corrected. MLD is calculated from glider CTD profiles according to the method of *Holte and Talley* [2009].

2.5 Used metrics (definitions)

The paper uses two metrics: a) model-to-observation bias (ΔQ_{mo}) defined as

$$\Delta Q_{mo} = \overline{Q(\text{model})} - \overline{Q(\text{observations})} \tag{1}$$

and b) Bias-Corrected Root Mean Square Difference (BC RMSD, $\Delta_{RD} Q_{mo}$) defined as

$$\Delta_{RD} Q_{mo} = \sqrt{\overline{(Q(\text{model}) - Q(\text{observations}) - \Delta Q_{mo})^2}} \ . \tag{2}$$

To compare the model with the observations, the observations were mapped into the model domain (each observation location to the nearest model grid point) and an average value was taken when multiple observations corresponded to the same model grid point.

It should be noted that the metrics from Eq.1-2 are used to measure "the skill" of the assimilative runs by comparing the simulation outputs to the assimilated data, rather than to an independent validation data-set. There are two reasons for this: firstly, to get sufficient validation data for the limited spatio-temporal region of this study is nearly impossible, however, most importantly, this study has no ambition to produce a skill-assessed reanalysis, its ambition is to test the impact of the assimilative system components on the simulated variables. Since the NEMOVAR reanalyses tend to converge under optimal conditions to the assimilated observations (*Skákala et al.* [2018, 2020]), the performance of the assimilative system can be measured by comparing the model to the assimilated data.

3 Results and Discussion

Fig.2 shows chlorophyll concentrations in the region measured by the glider between May and August 2018. The results shown in Fig.2 are consistent with previous studies (*Skákala et al.* [2018, 2020]): the NEMO-FABM-ERSEM model on the NWE Shelf shows a late and intense spring bloom (starting and peaking in May), whilst the satellite OC and in situ observations have spring bloom about 1 month earlier than the model (see *Skákala et al.* [2020]). When the assimilation starts in early May (Fig.2), the glider is in the post-bloom period showing some deep chlorophyll maxima, whereas the model free run has yet to see the onset of the bloom with chlorophyll concentrations predominantly in the mixed layer. Since the North Atlantic sees substantial seasonal patterns in primary productivity (e.g. *Henson et al.* [2009]), the late and intense model bloom has a large impact on the biogeochemical model skill.

In Fig.3 we address the impact of physical-only (temperature and salinity) assimilation on the model biogeochemistry. It is shown that the physical reanalysis improves the model representation of both temperature and salinity (Fig.3). As the pycnocline is primarily controlled by temperature and salinity, we expect that assimilating those variables may improve vertical gradients in water density and consequently vertical mixing. However, much of the vertical mixing in the upper oceanic layer is controlled by the atmospheric wind stress, which is provided as an external model input. In the well-mixed nutrient-rich waters the onset of the spring bloom depends on the interplay between vertical mixing in the upper oceanic layer and the underwater light (e.g. *Huisman et al.* [1999]; *Waniek* [2003]; *Smyth et al.* [2014]). Such interplay is closely related to the model atmospheric forcing, but even greater issue is the model response to the used atmospheric forcing, which consists here mostly of the ERSEM underwater light attenuation, the phytoplankton response to specific light conditions and the model vertical mixing scheme. The ERSEM response to the atmospheric forcing is known to be sensitive to the forcing temporal resolution, leading to important shifts in the timing of the phytoplankton bloom (*Powley et al.*

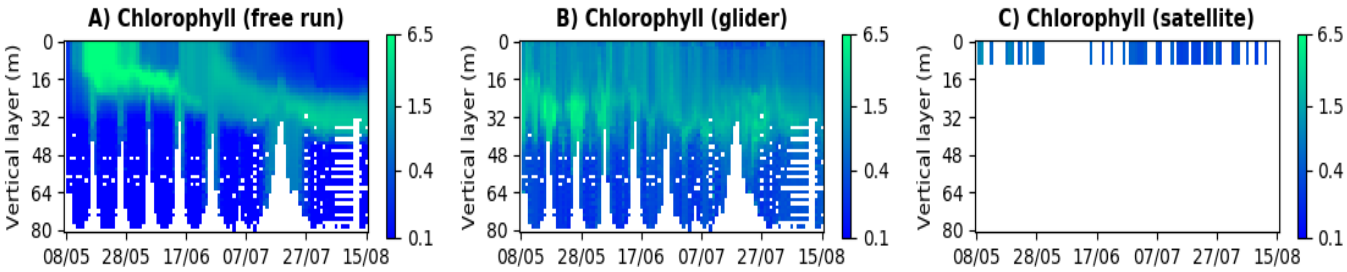

Figure 2. The Figure shows Hovmöller diagrams for the model free run and the observations. The left panel (A) shows the model free run outputs for total chlorophyll *a* (mg/m^3) horizontally averaged through the area covered by the glider during each day (the plot is depth vs time). The middle panel (B) shows the same for the glider-observed chlorophyll concentrations and the right panel (C) shows the satellite OC chlorophyll observations at the glider locations. The satellite observations are plotted in the upper 10 m, which broadly corresponds to the satellite optical depth (*Skákala et al.* [2020]) and the several missing data are due to the cloud cover.

[2020]). Since neither the model forcing, nor the model response to the forcing, change with the assimilation, neither there is much change to the MLD (Fig.3:C), assimilating temperature and salinity was found to have very little impact on the model skill to simulate chlorophyll (see Fig.4:A,E). The Tab.1 shows that the impact of physical assimilation on the (daily, time series) BC RMSD was for chlorophyll negligible (< 2%). The relative impact of physical assimilation on the model bias appears slightly larger (Tab.1), but that is due to the small values of the model bias, rather than large impact of physical assimilation. However, the impact of temperature and salinity assimilation on the simulated phytoplankton could become more substantial within a strongly coupled system (*Goodliff et al.* [2019]). In such system we mutually update the biogeochemical and the physical increments within a balancing scheme, which could be ideally defined using a two-way coupled physical-biogeochemical model (e.g. *Lengaigne et al.* [2007]). Such development is planned on the NWE Shelf in the foreseeable future.

In Fig.5 we analyse the impact of different components of the assimilative system on the skill of the reanalysis in representing chlorophyll. In particular, Fig.5 shows what changes to the model free run are required to better match the glider observations and how these changes are carried through by the different components of the multi-platform system. The satellite OC chlorophyll reanalysis from Fig.5:B is skilled not only in representing surface chlorophyll concentrations (Fig.6), but also in estimating the chlorophyll vertical profiles. Because the glider moved on the model grid dominantly in the vertical dimension, the model skill to represent vertical profiles of glider chlorophyll can be quantified using the spatial BC RMSD (Fig.4:F and Tab.1). Comparison of the spatial BC RMSD between the satellite OC chlorophyll assimilation and the free run (Tab.1) has shown that the spatial BC RMSD was improved in satellite OC assimilation by 17%. This is an encouraging result, even if it is outperformed by the glider chlorophyll assimilation, which improves the spatial BC RMSD by 62% (Tab.1). The positive impact of satellite chlorophyll assimilation on the model representation of chlorophyll vertical profiles can be understood from relatively simple chlorophyll dynamics: The satellite-only assimilative run removes the intense late model bloom in May, removing chlorophyll from the mixed layer and increasing the light penetrating into the water column. Although the vertical length-scales used in the satellite OC assimilation update chlorophyll only inside the mixed layer, the increased underwater light combined with nutrient availability produces deep chlorophyll maxima around the pycnocline. Furthermore, the removal of the late (May) bloom in the satellite OC reanalysis means the assimilation also removes the grad-

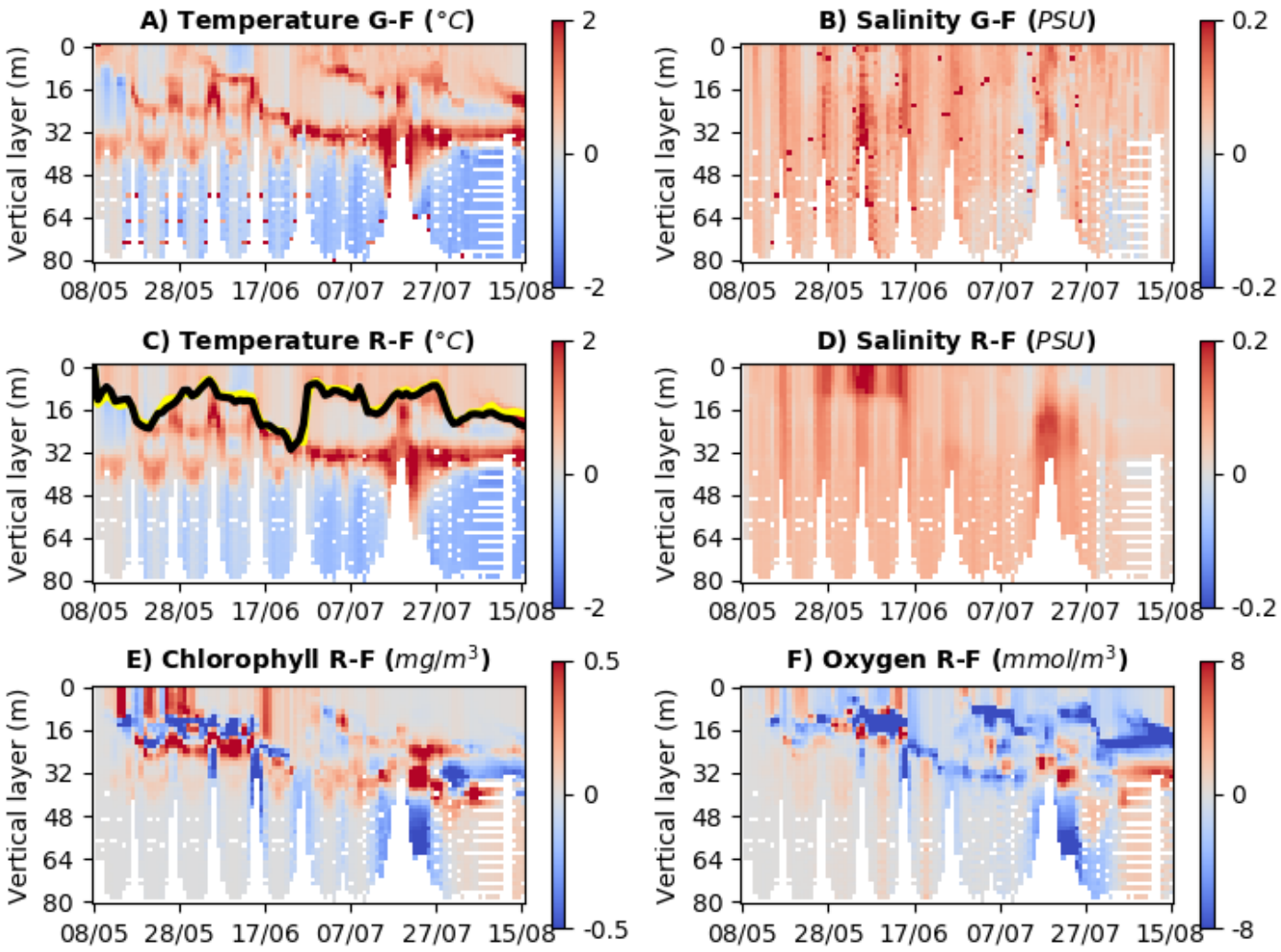

Figure 3. The Figure uses Hovmöller diagrams to demonstrate the impact of physical (temperature and salinity) assimilation on the model variables. The upper row (A and B) shows the difference between glider ("G" in the title) and free run ("F") outputs for temperature (A) and salinity (B). The middle row (C and D) shows differences for the same variables between physical reanalysis ("R") and the free run. The bottom row (E and F) shows the same differences between physical reanalysis and the free run, but for the two biogeochemical variables addressed by this study: total chlorophyll and oxygen. The two lines in the panel C mark the mixed layer depth of the free run (yellow) and of the physical reanalysis (black). The mixed layer depth has been obtained in both cases from the model outputs.

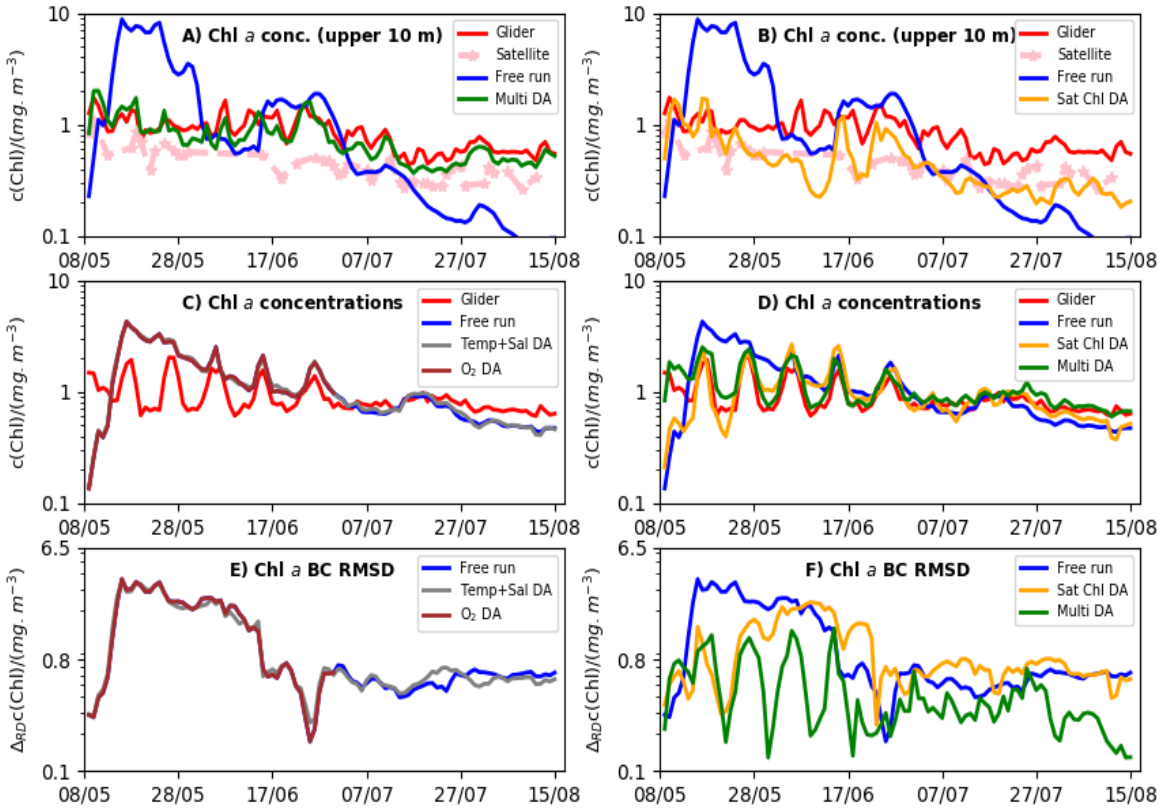

Figure 4. The Figure shows the impact of different multi-platform system components on the model chlorophyll concentrations. The panels A-B compare the daily chlorophyll values spatially averaged throughout the upper 10 meters of the water column, within the part of the model domain visited by the glider. The panels C-D show the daily values spatially averaged throughout the whole water column, within the part of the model domain visited by the glider (daily typically around 150 model grid points), and the remaining panels E-F show the daily BC RMSD (Eq.2) for the same part of the model domain than the panels C-D. The panels display the skill of the following system components: temperature and salinity assimilation (grey color), satellite OC chlorophyll assimilation (orange) and oxygen assimilation (brown). These components are compared with the multi-platform assimilative run (joint glider temperature-salinity-chlorophyll-oxygen and satellite OC chlorophyll assimilation, green color), the free run (blue), the glider observations (red) and the satellite OC data (pink).

Table 1. The Table demonstrates the skill measured by bias (Eq.1) and BC RMSD (Eq.2) of the free run and the relative (%) changes to the skill carried by the different assimilative system components. The skill compares the model simulations with the glider data. The "spatial BC RMSD" is just time-averaged value of the daily BC RMSD, i.e. calculated as a time-average from the 100 (chlorophyll), or 54 (oxygen) data points of the series shown in Fig.4:E-F and Fig.7:D. The "temporal BC RMSD" is the BC RMSD calculated from the time-series of the daily averages across all the spatial locations covered by the glider (the time series shown in Fig.4:A-D and Fig.7:A-C). The percentage changes in the columns for the assimilative runs are calculated relative to the free run skill. The negative percentage means that the bias, or BC RMSD is reduced by the specific system component, whilst the positive percentages mean that bias, or BC RMSD, increases.

variable	free run	temp+sal DA	sat Chl *a* DA	glid Chl *a* DA	O_2 DA	multi DA
Chl *a* bias	0.32 mg/m^3	+4.8%	-82.7%	-46.4%	0%	-42.2%
Chl *a* temporal BC RMSD	0.77 mg/m^3	+0.1%	-54.3%	-70.7%	0%	-71.9%
Chl *a* spatial BC RMSD	1.14 mg/m^3	-1.3%	-17.3%	-61.7%	0%	-60.4%
O_2 bias	-3.73 mmol/m^3	+25.7%	-59.2%	-27.8%	-81.7%	-86.9%
O_2 temporal BC RMSD	11.97 mmol/m^3	-2.7%	+13.8%	-0.3%	-42.3%	-55.2%
O_2 spatial BC RMSD	26.89 mmol/m^3	-4.3%	-7.9%	-12.8%	-37.1%	-47.1%

ually deepening chlorophyll maxima (the July-August period in Fig.2:B), as the nutrients become confined deeper in the water column. The satellite OC assimilation has a substantial impact on the (spatial mean) chlorophyll time series, improving the free run skill by more than 50% (temporal BC RMSD in Tab.1). There are two combined reasons for this improvement: the satellite OC data are reasonably consistent with the glider measurements (Fig.2, Fig.4:C-D), and the patterns in surface chlorophyll time series are a reasonable proxy for the time series of the vertically averaged chlorophyll concentrations.

Comparison between Fig.5:C and Fig.5:D shows that the chlorophyll concentrations around the glider locations are very similar between the multi-platform reanalysis (Fig.5:D) and the glider chlorophyll assimilation (Fig.5:C). This confirms that near the glider locations the glider chlorophyll assimilation is by far the most essential component of the multi-platform system in representing chlorophyll. The horizontal impact of glider assimilation (e.g. Fig.1) depends on the horizontal correlation length-scales and on the propagation of the assimilation increments with the advection. The Fig.8 shows that the impact of the glider assimilation on the reanalysis is mostly constrained within a 100 km horizontal radius, with the dominant part of the impact constrained within 30-50 km around the glider. The satellite assimilation has little impact on the multi-platform reanalysis near the glider locations, but plays naturally a major role in the regions away from the glider locations, where it substantially improves surface chlorophyll (Fig.6) and, as previously noted, improves chlorophyll vertical profiles (Fig.5). Both the multi-platform and glider chlorophyll assimilative runs lead to a major improvement in model skill to represent chlorophyll near the glider locations (Fig.4:B,F), with spatial BC RMSD improved by more than 70% and the temporal BC RMSD by more than 60% (Tab.1). Finally, we have observed that assimilating glider oxygen into the model has a negligible impact on the simulated chlorophyll concentrations, with a change to the skill metrics of the order $O(10^{-2})$ percent (Tab.1, see also Fig.4:A,E). This is expected, as the modeled oxygen influences phytoplankton concentrations only indirectly through a complex chain of marine

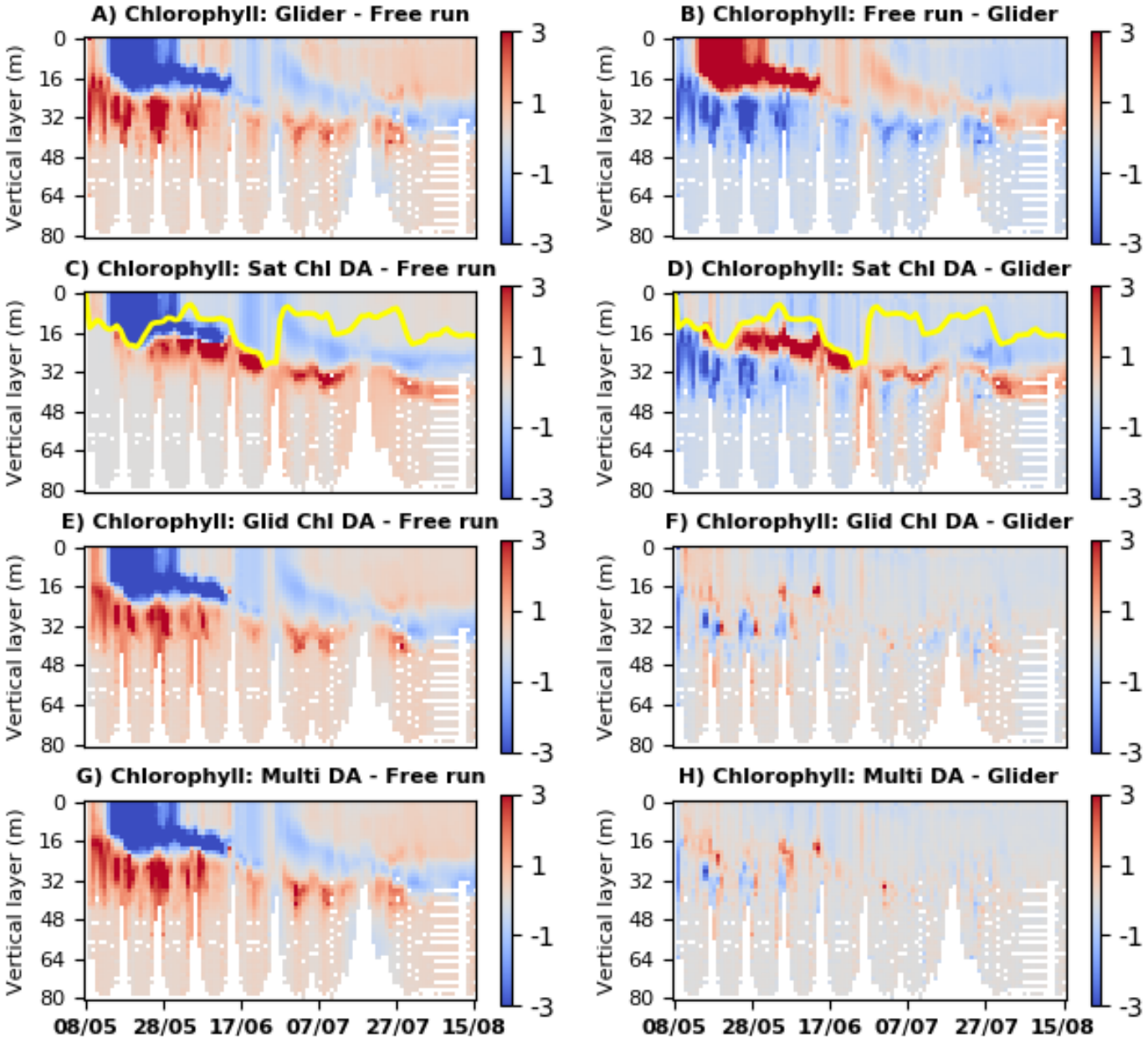

Figure 5. The left hand panels (A,C,E,G) demonstrate the impact of the multi-platform system components on the simulated chlorophyll *a* concentrations (mg/m^3) by comparing different simulations to the free run. The right hand panels (B,D,F,H) show the skill of each component by comparing the simulations to the glider observations. The first row shows the skill of the free run (panel B) and the required changes to the free run in order to better match the glider observations (panel A). The rows beneath the first row compare the chosen reference (free run or glider) with a range of system components: i) the reanalysis assimilating satellite OC chlorophyll (panels C and D), ii) the reanalysis assimilating glider chlorophyll (panels E and F) and iii) the multi-platform assimilation (joint glider temperature-salinity-chlorophyll-oxygen and satellite chlorophyll assimilation, panels G and H). The OC chlorophyll assimilation updates the model only within the mixed layer whose depth is marked by a yellow line (panels C and D).

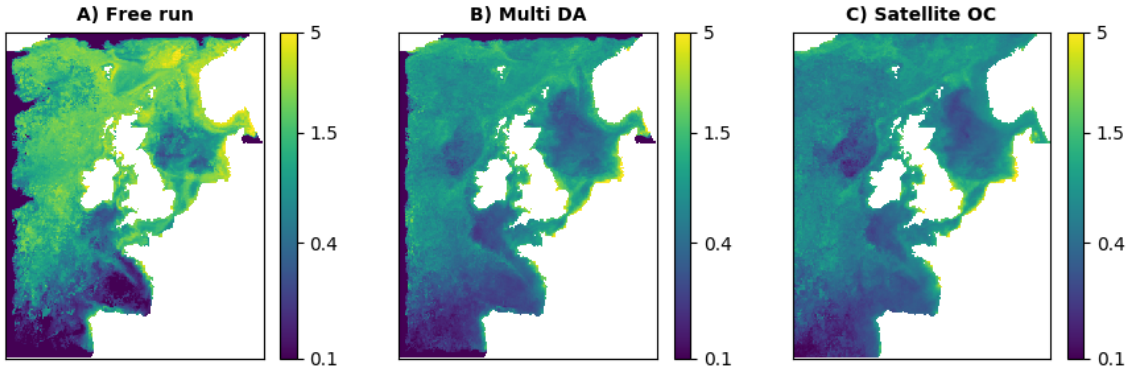

Figure 6. Comparison of the time median surface chlorophyll distributions (mg/m^3) for the simulation period (08/05/2018 - 15/08/2018). The three panels compare the free run (left panel), the multi-platform assimilation (middle panel) and the satellite distributions (right panel). It is shown that the multi-platform reanalysis is very similar to the assimilated satellite data on the whole NWE Shelf.

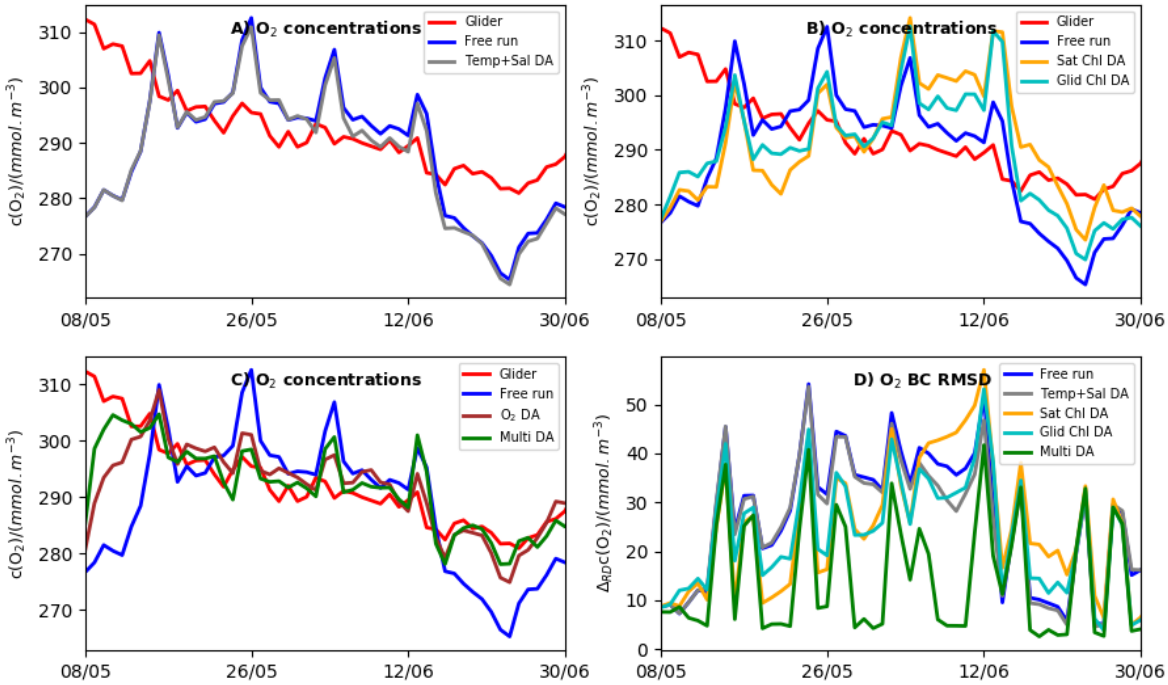

Figure 7. The Figure shows the impact of different multi-platform system components on the model oxygen. The panels A-C compare the daily oxygen values spatially averaged throughout the whole water column, within the part of the model domain visited by the glider (daily typically around 150 model grid points), and the panel D shows the daily BC RMSD (Eq.2). The panels display the skill of the following system components: temperature and salinity assimilation (grey color), satellite OC chlorophyll assimilation (orange), glider chlorophyll assimilation (light blue) and oxygen assimilation (brown). These components are compared with the multi-platform assimilative run (joint glider temperature-salinity-chlorophyll-oxygen and satellite chlorophyll assimilation, green color), the free run (blue) and the glider observations (red).

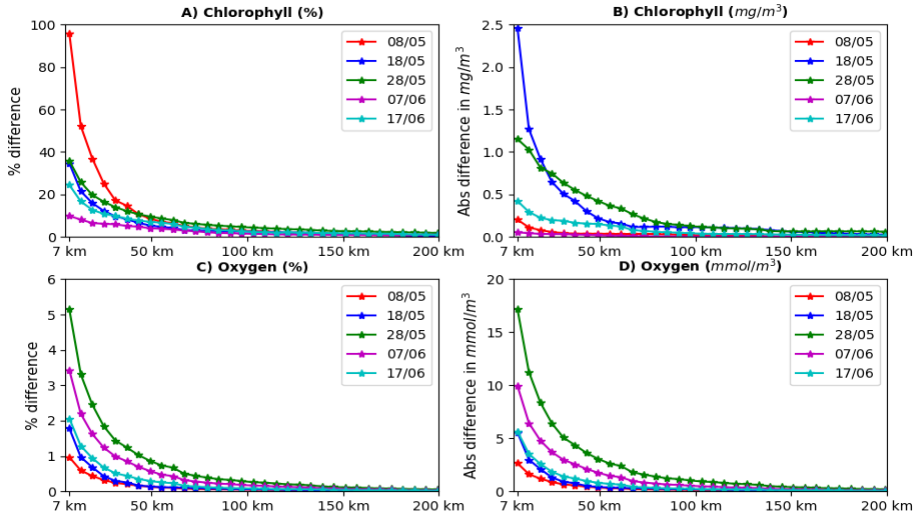

Figure 8. The Figure shows the horizontal scales for the impact of the glider chlorophyll (panels A-B) and the glider oxygen (panels C-D) assimilation. The impact of glider assimilation is shown for a range of days (between 08/05-17/06/2018). The impact is calculated by comparing the mean absolute value of the difference in chlorophyll (A-B panels), or oxygen (panels C-D) concentration between the reanalysis and the model free run. The mean absolute difference is shown relative to the free run values (in %, panels A,C), or in the absolute values (panels B,D). The absolute difference was averaged on the circles with 7-200 km radii (the spatial scales shown on the x-axis). The circles were centered around the glider daily mean location.

chemical and biological processes (e.g. through influencing remineralization, or nitrification rates, and through the impact of hypoxia on zooplankton).

Fig.9 shows a discrepancy between the oxygen time series of the glider and the model free run (see also Fig.10:A-B), with glider oxygen concentrations steadily decreasing (Fig.7:A), while the simulated oxygen peaks in the late May (Fig.7:A). Fig.7:A clearly shows that photosynthesis is an important driver of the simulated oxygen, producing a large oxygen surge in the mixed layer during the simulated late spring bloom. Some connection between oxygen and chlorophyll concentrations (a proxy for primary productivity) appears also in the glider observations (Fig.9), with the peak in oxygen concentrations located in the neighborhood of the glider deep chlorophyll maxima (Fig.2:B). Since the modeled oxygen concentrations are largely driven by the phytoplankton seasonal cycle, it is not surprising that assimilation of either satellite OC, or glider chlorophyll, has a major influence on the simulated oxygen (Fig.10:C,E). The assimilated chlorophyll modifies the simulated oxygen after a necessary time-lag, removing the excess oxygen from the model spring bloom and generating some deep oxygen maxima in the early-to-mid June (Fig.10:C-F). The chlorophyll assimilation consistently improves oxygen in the period up to the start of June, but sometimes degrades oxygen in the early-to-mid June (Fig.5:B,D, Fig.10:D,F), mostly due to the surge in oxygen concentrations around the deep oxygen maxima. The oxygen surge is likely to be partly driven by the deep chlorophyll maxima, e.g. by the overestimated chlorophyll concentrations around the deep maxima in the OC assimilation (Fig.5:D and Fig.4:B,F). However, the photosynthesis around the deep chlorophyll maxima cannot explain why the glider chlorophyll assimilation degrades the oxygen concentrations in the early June, i.e. why the simulated oxygen surges (Fig.7:B) while the glider assimilation mostly lowers the simulated chlorophyll (Fig.4:D). A further ex-

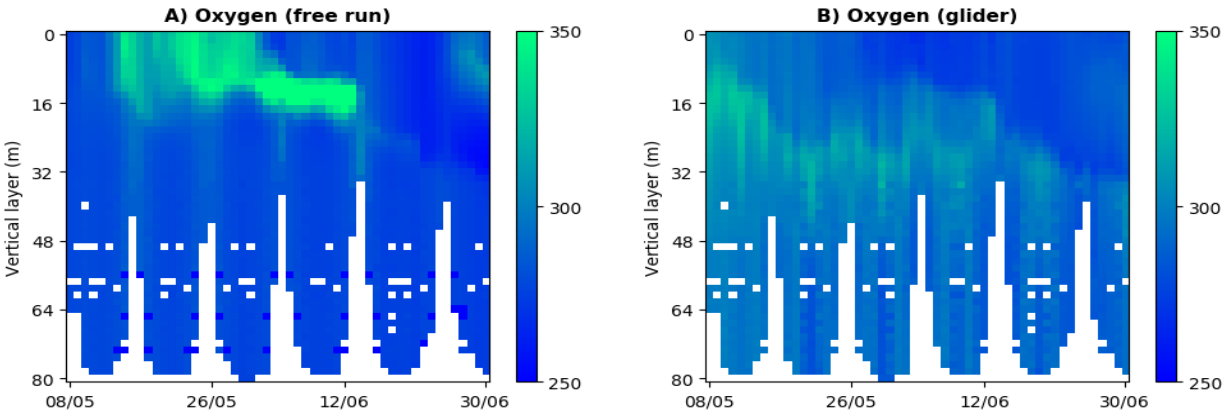

517 **Figure 9.** The Figure shows Hovmöller diagrams for the model free run and the glider observations. The
518 left panel (A) shows the model free run outputs for oxygen ($mmol/m^3$) horizontally averaged through the area
519 covered by the glider during each day (the plot is depth vs time). The right panel (B) shows the same for the
520 glider-observed oxygen.

497 planation for the deep oxygen maxima is given by Fig.11: the chlorophyll assimilation
498 removes the phytoplankton biomass from the mixed layer, which limits the resources for
499 the simulated zooplankton and bacteria, and reduces their concentrations (Fig.11:C-F).
500 The reduced phytoplankton concentrations seem to have much larger and more consistent
501 impact on the zooplankton concentrations than on bacteria (Fig.11:C-F). The reduced zoo-
502 plankton concentration means less oxygen is removed through respiration and this leaves
503 the excess simulated oxygen concentrations at the deep oxygen maxima (Fig.10:D,F). The
504 degradation in the modelled oxygen concentrations around the early June (e.g. Fig.7:B)
505 reminds us that ERSEM skill to simulate oxygen is too-complex to be fully addressed by
506 assimilating glider chlorophyll. For example, the temperature and salinity data assimilation
507 has a moderately larger (mostly positive) impact on the oxygen than on the chlorophyll
508 (Tab.1, Fig.7:A,D), which can be explained by the lowered oxygen saturation concentra-
509 tions (Fig.7:A) under the increase in temperature within the reanalysis (Fig.3:C). As for
510 chlorophyll, a simple way to improve simulated oxygen is to assimilate the glider oxygen
511 data into the model (Fig.10:D). Assimilating oxygen into the model reduces the spatial
512 BC RMSD by 35-50% (Tab.1) and the temporal BC RMSD by 40-55%, depending on
513 whether oxygen was the only assimilated variable, or as a part of multi-platform assim-
514 ilation (Tab.1). The multi-platform assimilation performs slightly better than the glider
515 chlorophyll component (Tab.1, Fig.7:C-D), presumably because by correcting the chloro-
516 phyll variable it improves the internal consistency of the analysis state.

536 ## 4 Summary

537 Present and future glider missions on the NWE Shelf will provide us with three-
538 dimensional (3D) data on some specific biogeochemical variables (presently mostly for
539 chlorophyll and oxygen) combined with physical measurements (e.g. temperature and
540 salinity). These data will be, together with satellite OC missions, integrated into our ecosys-
541 tem models by means of a multi-platform assimilative system. It is of crucial importance
542 to understand what observed variables need to be assimilated in order to represent well a
543 target ecosystem indicator, and what assimilation needs to be avoided because it can para-
544 doxically degrade the model skill for the target indicator. Furthermore, different data will
545 be available for different spatial and temporal regions on the NWE Shelf and it is essen-

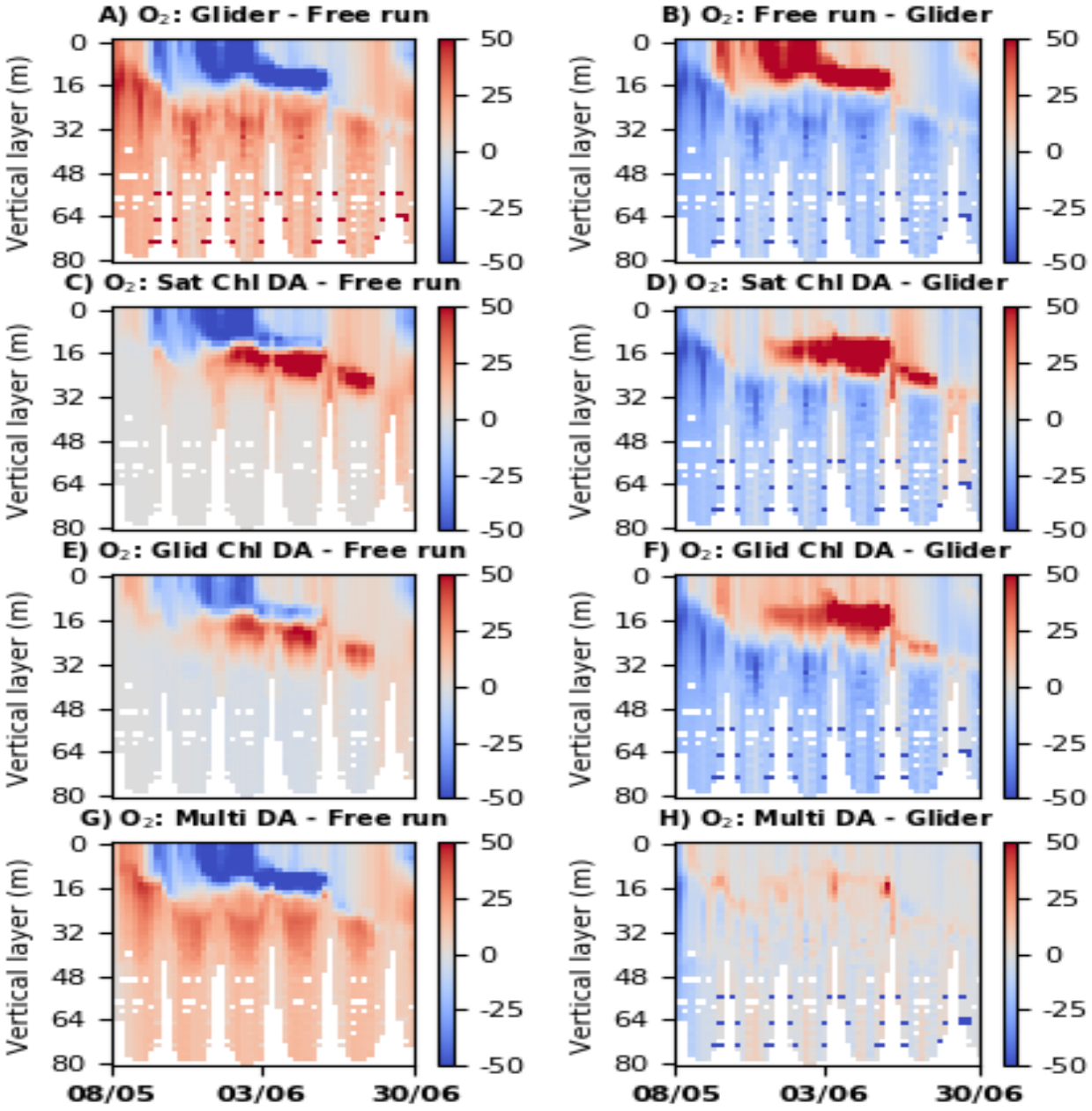

Figure 10. The left hand panels (A,C,E,G) demonstrate the impact of the multi-platform system components on the simulated oxygen concentrations ($mmol/m^3$) by comparing different simulations to the free run. The right hand panels (B,D,F,H) show the skill of each component by comparing the simulations to the glider observations. The first row shows the skill of the free run (panel B) and the required changes to the free run in order to better match the glider observations (panel A). The rows beneath the first row compare the chosen reference (free run or glider) with a range of system components: i) the reanalysis assimilating satellite OC chlorophyll (panels C and D), ii) the reanalysis assimilating glider chlorophyll (panels E and F) and iii) the multi-platform assimilation (joint glider temperature-salinity-chlorophyll-oxygen and satellite chlorophyll assimilation, panels G and H).

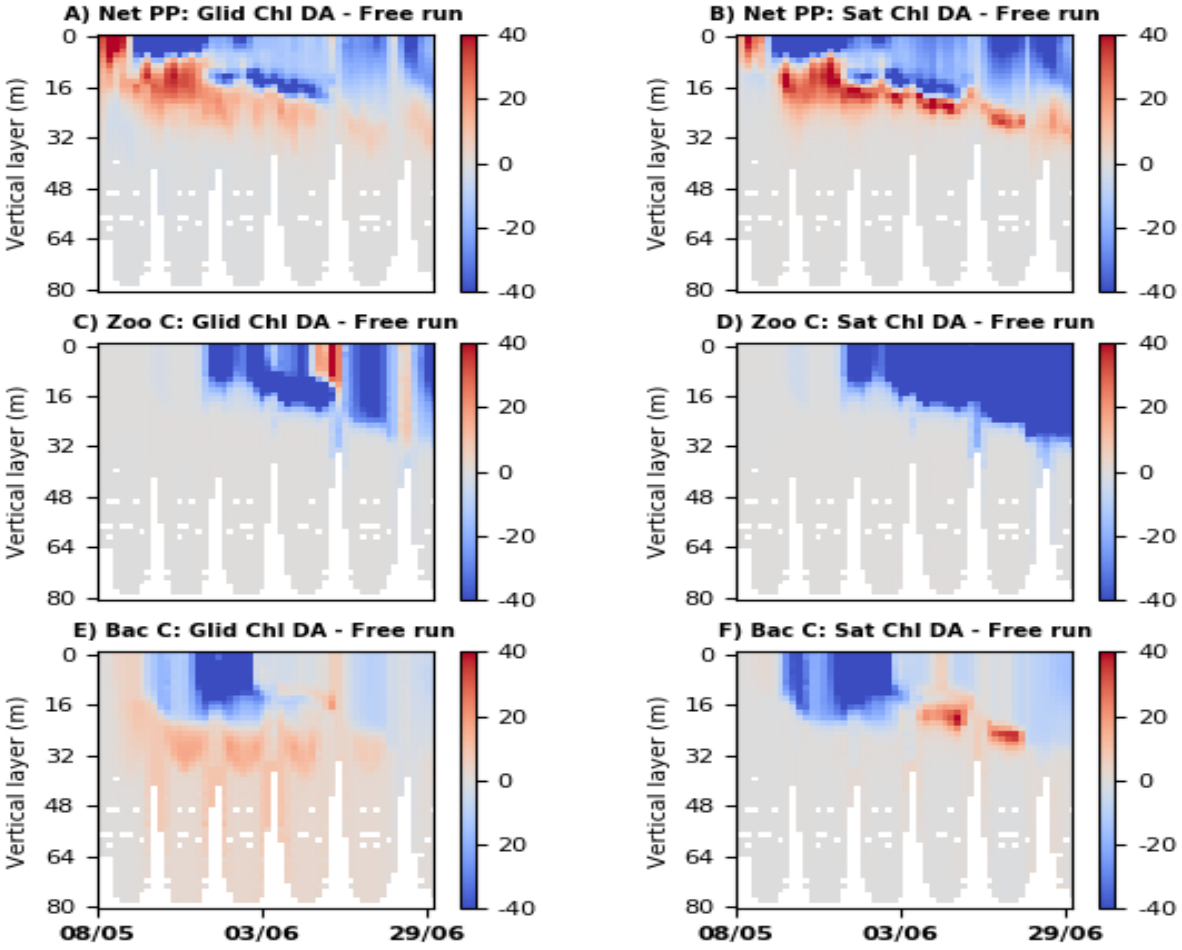

Figure 11. The Figure helps to interpret the impact of the simulated primary production and respiration on the modeled oxygen concentrations. We show the difference between the glider chlorophyll assimilation (left-hand side panels, A,C,E), or OC chlorophyll assimilation (right-hand side panels, B,D,F) and the model free run (always assimilative run minus free run). The difference is shown for (i) the total net primary production ($mg.C.m^{-3}.\text{day}^{-1}$, panels A-B), (ii) total zooplankton carbon concentrations ($mg.C/m^3$, panels C-D) and (iii) heterotrophic bacteria carbon concentrations ($mg.C/m^3$, panels E-F).

tial to understand how the limitations imposed by the availability of the observational data impact on the quality of the multi-platform reanalyses. To address these questions we explored the impact of different system components (glider physics, chlorophyll, oxygen and satellite OC chlorophyll assimilation) on future multi-platform reanalyses based on a current operational set-up used to assimilate satellite OC chlorophyll (*Skákala et al.* [2018, 2020]). This study has taught us several important lessons:

a) Assimilating physical glider data (temperature and salinity) improves the assimilated physical variables, but has negligible impact on the simulated phytoplankton bloom. This is because the modeled phytoplankton bloom depends in the North Sea mostly on the model response to the atmospheric forcing (wind stress and solar radiance), which remains unchanged by the temperature and salinity assimilation. Since the phytoplankton bloom is an essential driver of the ecosystem dynamics on the NWE Shelf (*Henson et al.* [2009]), it is reasonable to expect that physical glider data assimilation will not have a major importance for the simulated ecosystem dynamics on the NWE Shelf. This is quite different from some other global regions where physical assimilation is either desirable (*Anderson et al.* [2000]; *Yu et al.* [2018]), or can degrade the biogeochemical model skill (*Berline et al.* [2007]; *Holt et al.* [2014]; *Raghukumar et al.* [2015]; *Park et al.* [2018]). Based on this study we would suggest that, at least around the spring bloom in the North Sea, physical assimilation can be used to improve the physical model skill, without any need to worry about the coupled biogeochemical model.

b) The glider chlorophyll assimilation is within the 30-50 km horizontal proximity of the glider the dominant and most skilled component of the multi-platform system. Further away from the glider locations, assimilating satellite OC data has not only a major positive impact on the surface chlorophyll, but it can also improve the vertical chlorophyll profiles. Since satellite OC assimilation updates chlorophyll only within the mixed layer, the improvement in chlorophyll across the whole water column is explained by the model dynamical response to the assimilation. The skill of satellite OC assimilation in vertical chlorophyll is an encouraging result, as glider technology will be able to cover only limited parts of the NWE Shelf and future multi-platform assimilative system will have to rely heavily on satellite data.

c) The modelled phytoplankton dynamics is impacted by the oxygen concentrations only indirectly, e.g. through remineralization, or nitrification rates and the impact of hypoxia on zooplankton (*Butenschön et al.* [2016]). It is therefore not surprising that univariate assimilation of oxygen has a negligible impact on the simulated phytoplankton chlorophyll concentrations. This also means that one can assimilate oxygen into ERSEM without worrying about its consequences for the modelled phytoplankton. Such an oxygen assimilation has an obvious advantage in that it outperforms any other run in the model simulation of oxygen.

d) The simulated oxygen concentrations are largely driven by the primary production during the phytoplankton bloom. Consequently, assimilating (satellite OC, or glider) chlorophyll was found to have a major impact on the modeled oxygen. The removal of the late model bloom in the reanalysis improves the modeled oxygen, however it produces spurious deep oxygen maxima, partly due to the reduced respiration by the ERSEM zooplankton.

e) The multi-platform assimilation (joint glider temperature-salinity-chlorophyll-oxygen and satellite OC chlorophyll) combines optimally the skill of its components and always performs comparably to, or better than its best performing component.

f) Based on the results of this study we expect that the multi-platform system will provide us with improved-quality operational products on the NWE Shelf.

Acknowledgments

This work was supported by a joint effort of Natural Environment Research Council (NERC) funded projects of the Marine Integrated Autonomous Observing Systems (MIAOS) programme: Combining Autonomous observations and Models for Predicting and Understanding Shelf seas (CAMPUS) and Alternative Framework to Assess Marine Ecosystem Functioning in Shelf Seas (AlterECO, *http://projects.noc.ac.uk/altereco/*), grant no. NE/P013899/1. The work also benefited from the Copernicus Marine Environment Monitoring Service (CMEMS) funded projects OPTIcal data Modelling and Assimilation (OPTIMA) and NOWMAPS. We thank the European Space Agency Climate Initiative "Ocean Color" (http://www.esa-oceancolor-cci.org) for providing the ocean color data. The model was forced by atmospheric ERA-5 product of The European Centre for Medium-Range Weather Forecasts (ECMWF, *https://www.ecmwf.int/*). The river forcing data used by the model were prepared by Sonja van Leeuwen and Helen Powley as part of UK Shelf Seas Biogeochemistry programme (contract no. NE/K001876/1) of the NERC and the Department for Environment Food and Rural Affairs (DEFRA). We acknowledge use of the MONSooN system, a collaborative facility supplied under the Joint Weather and Climate Research Programme, a strategic partnership between the Met Office and the NERC. The different outputs for the free run simulations and reanalyses are stored on the MONSooN storage facility MASS and can be obtained upon request.

References

Allen, J., M. Eknes, and G. Evensen (2003), An ensemble kalman filter with a complex marine ecosystem model: hindcasting phytoplankton in the cretan sea, in *Annales Geophysicae*, vol. 21, pp. 399–411.

Anderson, L. A., A. R. Robinson, and C. J. Lozano (2000), Physical and biological modeling in the gulf stream region:: I. data assimilation methodology, *Deep Sea Research Part I: Oceanographic Research Papers*, *47*(10), 1787–1827.

Andersson, E. (2003), Modelling the temporal evolution of innovation statistics, *This volume*, pp. 153–164.

Artioli, Y., J. C. Blackford, M. Butenschön, J. T. Holt, S. L. Wakelin, H. Thomas, A. V. Borges, and J. I. Allen (2012), The carbonate system in the north sea: Sensitivity and model validation, *Journal of Marine Systems*, *102*, 1–13.

Baretta, J., W. Ebenhöh, and P. Ruardij (1995), The european regional seas ecosystem model, a complex marine ecosystem model, *Netherlands Journal of Sea Research*, *33*(3-4), 233–246.

Baretta-Bekker, J., J. Baretta, and W. Ebenhöh (1997), Microbial dynamics in the marine ecosystem model ersem ii with decoupled carbon assimilation and nutrient uptake, *Journal of Sea Research*, *38*(3-4), 195–211.

Bell, M. J., A. Schiller, P.-Y. Le Traon, N. Smith, E. Dombrowsky, and K. Wilmer-Becker (2015), An introduction to godae oceanview.

Berline, L., J.-M. Brankart, P. Brasseur, Y. Ourmières, and J. Verron (2007), Improving the physics of a coupled physical–biogeochemical model of the north atlantic through data assimilation: Impact on the ecosystem, *Journal of Marine Systems*, *64*(1-4), 153–172.

Biermann, L., C. Guinet, M. N. Bester, A. Brierley, and L. Boehme (2015), An alternative method for correcting fluorescence quenching.

Blackford, J. (1997), An analysis of benthic biological dynamics in a north sea ecosystem model, *Journal of Sea Research*, *38*(3-4), 213–230.

Borges, A., L.-S. Schiettecatte, G. Abril, B. Delille, and F. Gazeau (2006), Carbon dioxide in european coastal waters, *Estuarine, Coastal and Shelf Science*, *70*(3), 375–387.

Bruggeman, J., and K. Bolding (2014), A general framework for aquatic biogeochemical models, *Environmental modelling & software*, *61*, 249–265.

Butenschön, M., J. Clark, J. N. Aldridge, J. I. Allen, Y. Artioli, J. Blackford, J. Bruggeman, P. Cazenave, S. Ciavatta, S. Kay, et al. (2016), Ersem 15.06: a generic model for marine biogeochemistry and the ecosystem dynamics of the lower trophic levels, *Geoscientific Model Development*, *9*(4), 1293–1339.

Campbell, J. W. (1995), The lognormal distribution as a model for bio-optical variability in the sea, *Journal of Geophysical Research: Oceans*, *100*(C7), 13,237–13,254.

Carmillet, V., J.-M. Brankart, P. Brasseur, H. Drange, G. Evensen, and J. Verron (2001), A singular evolutive extended kalman filter to assimilate ocean color data in a coupled physical–biochemical model of the north atlantic ocean, *Ocean Modelling*, *3*(3-4), 167–192.

Ciavatta, S., R. Torres, S. Saux-Picart, and J. I. Allen (2011), Can ocean color assimilation improve biogeochemical hindcasts in shelf seas?, *Journal of Geophysical Research: Oceans*, *116*(C12).

Ciavatta, S., R. Torres, V. Martinez-Vicente, T. Smyth, G. Dall'Olmo, L. Polimene, and J. I. Allen (2014), Assimilation of remotely-sensed optical properties to improve marine biogeochemistry modelling, *Progress in oceanography*, *127*, 74–95.

Ciavatta, S., S. Kay, S. Saux-Picart, M. Butenschön, and J. Allen (2016), Decadal reanalysis of biogeochemical indicators and fluxes in the north west european shelf-sea ecosystem, *Journal of Geophysical Research: Oceans*, *121*(3), 1824–1845.

Ciavatta, S., R. Brewin, J. Skakala, L. Polimene, L. de Mora, Y. Artioli, and J. I. Allen (2018), Assimilation of ocean-color plankton functional types to improve marine ecosystem simulations, *Journal of Geophysical Research: Oceans*, *123*(2), 834–854.

Ciavatta, S., S. Kay, R. Brewin, R. Cox, A. Di Cicco, F. Nencioli, L. Polimene, M. Sammartino, R. Santoleri, J. Skákala, et al. (2019), Ecoregions in the mediterranean sea through the reanalysis of phytoplankton functional types and carbon fluxes, *Journal of Geophysical Research: Oceans*.

Cossarini, G., P. Lermusiaux, and C. Solidoro (2009), Lagoon of venice ecosystem: Seasonal dynamics and environmental guidance with uncertainty analyses and error subspace data assimilation, *Journal of Geophysical Research: Oceans*, *114*(C6).

Cossarini, G., L. Mariotti, L. Feudale, A. Mignot, S. Salon, V. Taillandier, A. Teruzzi, and F. D'Ortenzio (2019), Towards operational 3d-var assimilation of chlorophyll biogeochemical-argo float data into a biogeochemical model of the mediterranean sea, *Ocean Modelling*, *133*, 112–128.

Desroziers, G., L. Berre, B. Chapnik, and P. Poli (2005), Diagnosis of observation, background and analysis-error statistics in observation space, *Quarterly Journal of the Royal Meteorological Society: A journal of the atmospheric sciences, applied meteorology and physical oceanography*, *131*(613), 3385–3396.

Doney, S. C. (1999), Major challenges confronting marine biogeochemical modeling, *Global Biogeochemical Cycles*, *13*(3), 705–714.

Doney, S. C., K. Lindsay, K. Caldeira, J.-M. Campin, H. Drange, J.-C. Dutay, M. Follows, Y. Gao, A. Gnanadesikan, N. Gruber, et al. (2004), Evaluating global ocean carbon models: The importance of realistic physics, *Global Biogeochemical Cycles*, *18*(3).

El Moussaoui, A., C. Perruche, E. Greiner, C. Ethé, and M. Gehlen (2011), Integration of biogeochemistry into mercator ocean systems, *Mercator Océan Newsletter*, *40*, 3–14.

Fontana, C., C. Grenz, and C. Pinazo (2010), Sequential assimilation of a year-long time-series of seawifs chlorophyll data into a 3d biogeochemical model on the french mediterranean coast, *Continental Shelf Research*, *30*(16), 1761–1771.

Ford, D. (2020), Assimilating synthetic biogeochemical-argo and ocean colour observations into a global ocean model to inform observing system design, *submitted to Biogeosciences, freely available at https://www.biogeosciences-discuss.net/bg-2020-152/bg-2020-152.pdf*.

Ford, D., and R. Barciela (2017), Global marine biogeochemical reanalyses assimilating two different sets of merged ocean colour products, *Remote Sensing of Environment*, *203*, 40–54.

Ford, D., K. Edwards, D. Lea, R. Barciela, M. Martin, and J. Demaria (2012), Assimilating globcolour ocean colour data into a pre-operational physical-biogeochemical model, *Ocean Science*, *8*(5), 751–771.

Ford, D. A., J. van der Molen, K. Hyder, J. Bacon, R. Barciela, V. Creach, R. McEwan, P. Ruardij, and R. Forster (2017), Observing and modelling phytoplankton community structure in the north sea, *Biogeosciences*, *14*(6), 1419–1444.

Friedlingstein, P., P. Cox, R. Betts, L. Bopp, W. von Bloh, V. Brovkin, P. Cadule, S. Doney, M. Eby, I. Fung, et al. (2006), Climate–carbon cycle feedback analysis: results from the c4mip model intercomparison, *Journal of climate*, *19*(14), 3337–3353.

Garcia, H. E., R. A. Locarnini, T. P. Boyer, J. I. Antonov, O. K. Baranova, M. M. Zweng, J. R. Reagan, D. R. Johnson, A. V. Mishonov, and S. Levitus (2013), World ocean atlas 2013. volume 4, dissolved inorganic nutrients (phosphate, nitrate, silicate).

Geider, R., H. MacIntyre, and T. Kana (1997), Dynamic model of phytoplankton growth and acclimation: responses of the balanced growth rate and the chlorophyll a: carbon ratio to light, nutrient-limitation and temperature, *Marine Ecology Progress Series*, *148*, 187–200.

Germineaud, C., J.-M. Brankart, and P. Brasseur (2019), An ensemble-based probabilistic score approach to compare observation scenarios: an application to biogeochemical-argo deployments, *Journal of Atmospheric and Oceanic Technology*, (2019).

Goodliff, M., T. Bruening, F. Schwichtenberg, X. Li, A. Lindenthal, I. Lorkowski, and L. Nerger (2019), Temperature assimilation into a coastal ocean-biogeochemical model: assessment of weakly and strongly coupled data assimilation, *Ocean Dynamics*, *69*(10), 1217–1237.

Gregg, W. W. (2008), Assimilation of seawifs ocean chlorophyll data into a three-dimensional global ocean model, *Journal of Marine Systems*, *69*(3-4), 205–225.

Gregg, W. W., and C. S. Rousseaux (2017), Simulating pace global ocean radiances, *Frontiers in Marine Science*, *4*, 60.

Hemsley, V. S., T. J. Smyth, A. P. Martin, E. Frajka-Williams, A. F. Thompson, G. Damerell, and S. C. Painter (2015), Estimating oceanic primary production using vertical irradiance and chlorophyll profiles from ocean gliders in the north atlantic, *Environmental science & technology*, *49*(19), 11,612–11,621.

Henson, S. A., J. P. Dunne, and J. L. Sarmiento (2009), Decadal variability in north atlantic phytoplankton blooms, *Journal of Geophysical Research: Oceans*, *114*(C4).

Holt, J., J. I. Allen, T. R. Anderson, R. Brewin, M. Butenschön, J. Harle, G. Huse, P. Lehodey, C. Lindemann, L. Memery, et al. (2014), Challenges in integrative approaches to modelling the marine ecosystems of the north atlantic: Physics to fish and coasts to ocean, *Progress in Oceanography*, *129*, 285–313.

Holte, J., and L. Talley (2009), A new algorithm for finding mixed layer depths with applications to argo data and subantarctic mode water formation, *Journal of Atmospheric and Oceanic Technology*, *26*(9), 1920–1939.

Hoteit, I., G. Triantafyllou, G. Petihakis, and J. Allen (2003), A singular evolutive extended kalman filter to assimilate real in situ data in a 1-d marine ecosystem model.

Hoteit, I., G. Triantafyllou, and G. Petihakis (2005), Efficient data assimilation into a complex, 3-d physical-biogeochemical model using partially-local kalman filters.

Huisman, J., P. van Oostveen, and F. J. Weissing (1999), Critical depth and critical turbulence: two different mechanisms for the development of phytoplankton blooms, *Limnology and oceanography*, *44*(7), 1781–1787.

Ishizaka, J. (1990), Coupling of coastal zone color scanner data to a physical-biological model of the southeastern us continental shelf ecosystem: 2. an eulerian model, *Journal of Geophysical Research: Oceans*, *95*(C11), 20,183–20,199.

Jahnke, R. A. (2010), Global synthesis, in *Carbon and nutrient fluxes in continental margins*, pp. 597–615, Springer.

Johnson, K. (2016), The scientific rationale, design and implementation plan for a biogeochemical-argo float array, *Planning Group Rep.*

Johnson, K., and H. Claustre (2016), Bringing biogeochemistry into the argo age, *Eos*, *97*(10.1029).

Jones, E. M., M. E. Baird, M. Mongin, J. Parslow, J. Skerratt, J. Lovell, N. Margvelashvili, R. J. Matear, K. Wild-Allen, B. Robson, et al. (2016), Use of remote-sensing reflectance to constrain a data assimilating marine biogeochemical model of the great barrier reef, *Biogeosciences*, *13*(23), 6441–6469.

Kalaroni, S., K. Tsiaras, G. Petihakis, I. Hoteit, A. Economou-Amilli, and G. Triantafyllou (2016), Data assimilation of depth-distributed satellite chlorophyll-α in two mediterranean contrasting sites, *Journal of Marine Systems*, *160*, 40–53.

Key, R. M., A. Olsen, S. van Heuven, S. K. Lauvset, A. Velo, X. Lin, C. Schirnick, A. Kozyr, T. Tanhua, M. Hoppema, et al. (2015), Global ocean data analysis project, version 2 (glodapv2).

King, R. R., J. While, M. J. Martin, D. J. Lea, B. Lemieux-Dudon, J. Waters, and E. O'Dea (2018), Improving the initialisation of the met office operational shelf-seas model, *Ocean Modelling*, *130*, 1–14.

Lauvset, S. K., R. M. Key, A. Olsen, S. van Heuven, A. Velo, X. Lin, C. Schirnick, A. Kozyr, T. Tanhua, M. Hoppema, et al. (2016), A new global interior ocean mapped climatology: The 1× 1 glodap version 2, *Earth System Science Data*, *8*, 325–340.

Legge, O., M. Johnson, N. Hicks, T. Jickells, M. Diesing, J. Aldridge, J. Andrews, Y. Artioli, D. C. Bakker, M. T. Burrows, et al. (2020), Carbon on the northwest european shelf: Contemporary budget and future influences, *Frontiers in Marine Science*, *7*, 143.

Lellouche, J.-M., O. Le Galloudec, M. Drévillon, C. Régnier, E. Greiner, G. Garric, N. Ferry, C. Desportes, C.-E. Testut, C. Bricaud, et al. (2013), Evaluation of global monitoring and forecasting systems at mercator océan, *Ocean Science*, *9*(1), 57.

Lenartz, F., C. Raick, K. Soetaert, and M. Grégoire (2007), Application of an ensemble kalman filter to a 1-d coupled hydrodynamic-ecosystem model of the ligurian sea, *Journal of Marine Systems*, *68*(3-4), 327–348.

Lengaigne, M., C. Menkes, O. Aumont, T. Gorgues, L. Bopp, J.-M. André, and G. Madec (2007), Influence of the oceanic biology on the tropical pacific climate in a coupled general circulation model, *Climate Dynamics*, *28*(5), 503–516.

Lenhart, H.-J., D. K. Mills, H. Baretta-Bekker, S. M. Van Leeuwen, J. Van Der Molen, J. W. Baretta, M. Blaas, X. Desmit, W. Kühn, G. Lacroix, et al. (2010), Predicting the consequences of nutrient reduction on the eutrophication status of the north sea, *Journal of Marine Systems*, *81*(1-2), 148–170.

Lutz, M. J., K. Caldeira, R. B. Dunbar, and M. J. Behrenfeld (2007), Seasonal rhythms of net primary production and particulate organic carbon flux to depth describe the efficiency of biological pump in the global ocean, *Journal of Geophysical Research: Oceans*, *112*(C10).

Madec, G., et al. (2015), Nemo ocean engine.

Mogensen, K., M. Balmaseda, A. Weaver, M. Martin, and A. Vidard (2009), Nemovar: A variational data assimilation system for the nemo ocean model, *ECMWF newsletter*, *120*, 17–22.

Mogensen, K., M. A. Balmaseda, A. Weaver, et al. (2012), The nemovar ocean data assimilation system as implemented in the ecmwf ocean analysis for system 4.

Natvik, L.-J., and G. Evensen (2003), Assimilation of ocean colour data into a biochemical model of the north atlantic: Part 1. data assimilation experiments, *Journal of Marine Systems*, *40*, 127–153.

Nerger, L., and W. W. Gregg (2007), Assimilation of seawifs data into a global ocean-biogeochemical model using a local seik filter, *Journal of Marine Systems*, *68*(1-2), 237–254.

Nerger, L., and W. W. Gregg (2008), Improving assimilation of seawifs data by the application of bias correction with a local seik filter, *Journal of marine systems*, *73*(1-2), 87–102.

O'Dea, E., R. Furner, S. Wakelin, J. Siddorn, J. While, P. Sykes, R. King, J. Holt, and H. Hewitt (2017), The co5 configuration of the 7 km atlantic margin model: large-scale biases and sensitivity to forcing, physics options and vertical resolution, *Geoscientific Model Development*, *10*(8), 2947.

Oschlies, A., and V. Garçon (1999), An eddy-permitting coupled physical-biological model of the north atlantic: 1. sensitivity to advection numerics and mixed layer physics, *Global Biogeochemical Cycles*, *13*(1), 135–160.

Park, J.-Y., C. A. Stock, X. Yang, J. P. Dunne, A. Rosati, J. John, and S. Zhang (2018), Modeling global ocean biogeochemistry with physical data assimilation: a pragmatic solution to the equatorial instability, *Journal of Advances in Modeling Earth Systems*, *10*(3), 891–906.

Pauly, D., V. Christensen, S. Guénette, T. J. Pitcher, U. R. Sumaila, C. J. Walters, R. Watson, and D. Zeller (2002), Towards sustainability in world fisheries, *Nature*, *418*(6898), 689.

Powley, H. R., J. Bruggeman, J. Hopkins, T. Smyth, and J. Blackford (2020), Sensitivity of shelf sea marine ecosystems to temporal resolution of meteorological forcing, *Journal of Geophysical Research: Oceans*, p. e2019JC015922.

Pradhan, H. K., C. Völker, S. Losa, A. Bracher, and L. Nerger (2019), Assimilation of global total chlorophyll oc-cci data and its impact on individual phytoplankton fields, *Journal of Geophysical Research: Oceans*, *124*(1), 470–490.

Raghukumar, K., C. A. Edwards, N. L. Goebel, G. Broquet, M. Veneziani, A. M. Moore, and J. P. Zehr (2015), Impact of assimilating physical oceanographic data on modeled ecosystem dynamics in the california current system, *Progress in Oceanography*, *138*, 546–558.

Sathyendranath, S., R. J. Brewin, C. Brockmann, V. Brotas, B. Calton, A. Chuprin, P. Cipollini, A. B. Couto, J. Dingle, R. Doerffer, et al. (2019), An ocean-colour time series for use in climate studies: The experience of the ocean-colour climate change initiative (oc-cci), *Sensors*, *19*(19), 4285.

Shulman, I., S. Frolov, S. Anderson, B. Penta, R. Gould, P. Sakalaukus, and S. Ladner (2013), Impact of bio-optical data assimilation on short-term coupled physical, bio-optical model predictions, *Journal of Geophysical Research: Oceans*, *118*(4), 2215–2230.

Skákala, J., D. Ford, R. J. Brewin, R. McEwan, S. Kay, B. Taylor, L. de Mora, and S. Ciavatta (2018), The assimilation of phytoplankton functional types for operational forecasting in the northwest european shelf, *Journal of Geophysical Research: Oceans*, *123*(8), 5230–5247.

Skákala, J., J. Bruggeman, R. J. Brewin, D. A. Ford, and S. Ciavatta (2020), Improved representation of underwater light field and its impact on ecosystem dynamics: a study in the north sea, *Journal of Geophysical Research: Oceans*, p. e2020JC016122.

Smyth, T. J., I. Allen, A. Atkinson, J. T. Bruun, R. A. Harmer, R. D. Pingree, C. E. Widdicombe, and P. J. Somerfield (2014), Ocean net heat flux influences seasonal to interannual patterns of plankton abundance, *PloS one*, *9*(6).

Song, H., C. A. Edwards, A. M. Moore, and J. Fiechter (2016), Data assimilation in a coupled physical-biogeochemical model of the california current system using an incremental lognormal 4-dimensional variational approach: Part 3—assimilation in a realistic context using satellite and in situ observations, *Ocean Modelling*, *106*, 159–172.

Swart, S., S. J. Thomalla, and P. Monteiro (2015), The seasonal cycle of mixed layer dynamics and phytoplankton biomass in the sub-antarctic zone: A high-resolution glider experiment, *Journal of Marine Systems*, *147*, 103–115.

Telszewski, M., A. Palacz, and A. Fischer (2018), Biogeochemical in situ observations–motivation, status, and new frontiers, *New Frontiers in Operational Oceanography*, pp. 131–160.

Torres, R., J. Allen, and F. Figueiras (2006), Sequential data assimilation in an upwelling influenced estuary, *Journal of Marine Systems*, *60*(3-4), 317–329.

Triantafyllou, G., G. Korres, I. Hoteit, G. Petihakis, and A. Banks (2007), Assimilation of ocean colour data into a biogeochemical flux model of the eastern mediterranean sea.

Vaquer-Sunyer, R., and C. M. Duarte (2008), Thresholds of hypoxia for marine biodiversity, *Proceedings of the National Academy of Sciences*, *105*(40), 15,452–15,457.

Verdy, A., and M. Mazloff (2017), A data assimilating model for estimating s outhern o cean biogeochemistry, *Journal of Geophysical Research: Oceans*, *122*(9), 6968–6988.

Visbeck, M., M. Araujo, A. Boetius, E. Buch, H. Claustre, T. Dabrowski, E. Delory, B. de Young, K. Drinkwater, A. Fischer, et al. (2015), More integrated and more sustainable atlantic ocean observing (atlantos), *CLIVAR Exchanges*, *67*(2), 18–20.

Waniek, J. J. (2003), The role of physical forcing in initiation of spring blooms in the northeast atlantic, *Journal of Marine Systems*, *39*(1-2), 57–82.

Waters, J., D. J. Lea, M. J. Martin, I. Mirouze, A. Weaver, and J. While (2015), Implementing a variational data assimilation system in an operational 1/4 degree global ocean model, *Quarterly Journal of the Royal Meteorological Society*, *141*(687), 333–349.

While, J., K. Haines, and G. Smith (2010), A nutrient increment method for reducing bias in global biogeochemical models, *Journal of Geophysical Research: Oceans*, *115*(C10).

Xing, X., H. Claustre, S. Blain, F. d'Ortenzio, D. Antoine, J. Ras, and C. Guinet (2012), Quenching correction for in vivo chlorophyll fluorescence acquired by autonomous platforms: A case study with instrumented elephant seals in the kerguelen region (southern ocean), *Limnology and Oceanography: Methods*, *10*(7), 483–495.

Yu, L., K. Fennel, L. Bertino, M. El Gharamti, and K. R. Thompson (2018), Insights on multivariate updates of physical and biogeochemical ocean variables using an ensemble kalman filter and an idealized model of upwelling, *Ocean Modelling*, *126*, 13–28.